Title

Thyroid-specific inactivation of KIF3A alters the TSH signaling pathway and leads to hypothyroidism

Journal

Journal of Molecular Endocrinology, 50(3)

ISSN

0952-5041

Authors

D'Amico, Eva
Gayral, Stéphanie
Massart, Claude
et al.

Publication Date

2013-06-01

DOI

10.1530/jme-12-0219

Peer reviewed

HHS Public Access

Author manuscript

J Mol Endocrinol. Author manuscript; available in PMC 2015 April 21.

Published in final edited form as:

J Mol Endocrinol. 2013 June ; 50(3): 375–387. doi:10.1530/JME-12-0219.

Thyroid-specific inactivation of KIF3A alters TSH signaling pathway and leads to hypothyroidism

Eva D'Amico[1], **Stéphanie Gayral**[1], **Claude Massart**[2], **Jacqueline Van Sande**[2], **Jeremy F. Reiter**[3], **Jacques E. Dumont**[2], **Bernard Robaye**[1], and **Stéphane Schurmans**[1,4,5,6]

[1]Institut de Recherche Interdisciplinaire en Biologie Humaine et Moléculaire (IRIBHM), Institut de Biologie et de Médecine Moléculaires (IBMM), Université Libre de Bruxelles (ULB), rue des Professeurs Jeener et Brachet 12, 6041-Gosselies, Belgium

[2]IRIBHM, ULB, Campus Erasme, route de Lennik 808, 1070-Brussels, Belgium

[3]Department of Biochemistry and Biophysics, Smith Cardiovascular Research Building, Mission Bay Blvd South 555, University of California, San Francisco, San Francisco, CA 94158-9001, USA

[4]Laboratoire de Génétique Fonctionnelle, GIGA-Research Centre, Université de Liège (ULg), rue de 1'Hôpital 1, 4000-Liège, Belgium

[5]Welbio, ULg

[6]Secteur de Biochimie Métabolique, Département des Sciences Fonctionnelles, ULg, Boulevard de Colonster 20, 4000-Liège, Belgium

Abstract

Kinesins, including the kinesin 2/KIF3 molecular motor, play an important role in intracellular traffic and can deliver vesicles to distal axon terminal, to cilia, to non-polarized cell surface or to epithelial cell basolateral membrane, thus taking part to the establishment of cellular polarity. We report here the consequences of the kinesin 2 motor inactivation in the thyroid of 3 week-old $Kif3a^{\Delta/flox}$ $Pax8^{Cre/+}$ mutant mice. Our results indicate first that 3 week-old $Pax8^{Cre/+}$ mice used in these experiments present minor thyroid functional defects resulting in a slight increase in circulating bioactive TSH and intracellular cAMP levels, sufficient to maintain blood T4 levels in the normal range. Second, Kif3a inactivation in thyrocytes markedly amplified the phenotype observed in $Pax8^{Cre/+}$ mice, resulting in an altered TSH signaling upstream of the second messenger cAMP and mild hypothyroidism. Finally, our results in mouse embryonic fibroblasts

Corresponding author: Stéphane Schurmans, Laboratoire de Génétique Fonctionnelle, GIGA-Research Centre, Université de Liège, rue de 1'Hôpital 1, 4000-Liège, Belgium. Phone: +32 4 366.33.72; sschurmans@ulg.ac.be.

Declaration of interest: The authors declare that there is no conflict of interest that could be perceived as prejudicing the impartiality of the research reported.

Author contributions Eva D'Amico : Researched data, Contributed to discussion, Wrote manuscript
Stéphanie Gayral : Researched data
Claude Massart : Researched data
Jacqueline Van Sande : Contributed to discussion
Jeremy F. Reiter : Supplied material
Jacques E. Dumont : Contributed to discussion
Bernard Robaye : Contributed to discussion
Stéphane Schurmans : Designed project, Contributed to discussion, Wrote manuscript

indicate that Kif3a inactivation in the absence of any Pax8 gene alteration leads to altered GPCR plasma membrane expression, as shown for the β2 adrenergic receptor, and we suggest that a similar mechanism may explain the altered TSH signaling and mild hypothyroidism detected in $Kif3a^{\Delta/flox}$ $Pax8^{Cre/+}$ mutant mice.

Keywords

thyroid; hypothyroidism; genetically-modified mouse; Kif3a; molecular motor; kinesin 2

Introduction

Little is known about molecular motors responsible for intracellular traffic in thyroid follicle cells. However, like in other polarized cells, thyroid proteins must specifically reach the apical or basolateral membrane to be functional. In order to assure the synthesis of T3 and T4 thyroid hormones, the thyroid stimulating hormone (TSH) receptor and the sodium-iodide symporter (NIS) must reach the basolateral surface, while thyroperoxydase (TPO) and the dual oxidases (DUOXs) must be transported to the thyrocyte apical membrane, and thyroglobulin (TG) exported through the apical membrane in the colloid.

Kinesins play an important role in intracellular traffic. The superfamily of kinesins is constituted of motor proteins that use energy liberated from ATP hydrolysis to transport vesicles along microtubules. These proteins are composed of a motor domain containing an ATP binding site and a microtubule binding site, a domain which binds vesicles and an oligomerization domain (Scholey 1996). Most of these motor proteins, including kinesin 2, mediate vesicles transport over long distances to the plus-end of microtubules. This transport pathway is highly conserved through evolution. In view of microtubules organization, kinesins can deliver vesicles to distal axon terminal, to cilia or flagella, to non-polarized cell surface or to epithelial cell basolateral membrane, taking part to the establishment of cellular polarity (Hirokawa 2000). Kinesin 2 motor (or KIF3, kinesin family member 3) is composed of a heterotrimeric complex KIF3A-KIF3B-KAP3. KIF3A/B are the motor proteins and KAP3 regulates the binding between the cargo and the KIF3 heterodimer (Hirokawa 2000). This molecular motor is expressed in all tissues, including the thyroid. KIF3A or KIF3B inactivation in mice leads to abolition of molecular motor function and to an early embryonic lethality. These knockout embryos exhibit loss of cilia ordinarily present on cells of the embryonic node, leading to a randomized establishment of left-right asymmetry and numerous structural abnormalities (Nonaka *et al.* 1998; Marszalek *et al.* 1999).

In this study, we have explored the role of the kinesin 2 molecular motor in mouse thyroid development, structure and function 3 weeks after birth. We used mice carrying a Kif3a floxed gene as well as knock-in mice expressing the Cre recombinase under the control of the endogenous Pax8 promoter (Marszalek *et al.* 1999; Bouchard *et al.* 2004). Indeed, in these $Pax8^{Cre/+}$ mice, the expression of the recombinase mimics the expression of the paired-domain transcription factor Pax8, including thyroid follicle cells, kidney, inner ear and the mid-hindbrain boundary region, all of them from the embryonic stage E8.5 (Plachov *et al.* 1990; Bouchard *et al.* 2002).

Materials and methods

Mice

Kif3a$^{\Delta/flox}$ mice, obtained from L. S. Goldstein (University of California, San Diego, USA) and Pax8$^{Cre/+}$ mice, obtained from M. Busslinger (Research Institute of Molecular Pathology, Vienna, Austria) were on a mixed Sv129 x C56BL/6 genetic background. All procedures were approved by the Ethical Committee of the Medical and the Sciences School of the Université Libre de Bruxelles.

Genotyping and analysis of Cre/lox recombination specificity

PCR were performed on tail DNA with oligonucleotide primers 1 (5'-AGGGCAGACGGAAGGGTGG-3'), 2 (5'-TCTGTGAGTTTGTGACCAGCC-3') and 3 (5'-TGGCAGGTCAATGGACGCAG-3'). Using these three primers in the same PCR, amplicons of 200 bp, 360 bp and 490 bp were obtained, corresponding to the delta, wild-type and floxed Kif3a allele, respectively.

Cell Culture

Large T antigen-immortalized Kif3a$^{+/+}$ and Kif3a$^{-/-}$ mouse embryonic fibroblasts (MEFs) were maintained in Dulbecco's Modified Eagle Medium supplemented with 100 U/ml penicillin, 100 µg/ml streptomycin, 15% fetal bovine serum, 1.1 mM sodium pyruvate, 3.97 mM L-glutamine, 100 µM non-essential amino acids and 300 µg/ml G418 (Sigma-Aldrich, St. Louis, MO). Cells were kept in a humidified incubator at 37°C and 5% CO_2. The medium was changed every 3 days.

Western blotting

Thyroid and MEF proteins were extracted using RIPA buffer (Tris-Hcl 50 mM pH 7.4, EDTA 1 mM, NaCl 150 mM, Triton X-100 1%, Sodium deoxycholate 1%, SDS 0.1%). Thyroid (25 µg) and MEF (60 µg) protein extracts were separated on a 10% SDS-polyacrylamide gel and transferred to polyvinylidene difluoride membrane (Amersham Biosciences, Glattbrugg, Switzerland) using a Mini Trans-Blot Transfer Cell system (Bio-Rad). Membrane was preincubated for 1 h with 5% milk and 0.1% Tween in PBS, followed by overnight incubation at 4°C with a Kif3a antibody (Sigma-Aldrich, St. Louis, MO) diluted 1:2000, or with a beta actin antibody (Sigma-Aldrich, St. Louis, MO) diluted 1:5000, or with a β_2 adrenergic receptor antibody (AbCam, UK) diluted 1:1000 in the same buffer. The membrane was washed in PBS and then incubated for 1 h at room temperature with peroxidase-conjugated protein A (Sigma-Aldrich, St. Louis, MO) diluted 1:10,000. Proteins were visualized with Western Lightning plus-ECL (Perkin-Elmer) and exposure to x-ray film. Protein concentration was determined with Bio-Rad protein assay reagents using BSA as standard.

Serum hormone assays

Enzyme Immunoassays for mouse T3 and T4 were performed using Mouse/Rat T3 ELISA kit from Calbiotech (Spring Valley, Canada) and T4 ELISA kit from DiaSource (Louvain-La-Neuve, Belgium), respectively. TSH was measured in a bioassay using a line of Chinese

hamster ovary (CHO) cells stably transfected with the human TSH receptor cDNA, as previously described (Perret *et al.* 1990; Moeller *et al.* 2003). Briefly, 50,000 cells were seeded in individual test tubes and incubated for 24 h in 100 µl Ham's F-12 nutrient mixture supplemented with 10% fetal calf serum, 100 IU/ml penicillin, 100 µg/ml streptomycin, 1 mM sodium pyruvate and 2.5 µg/ml Fungizone. Cells were washed with 500 µl Krebs Ringer HEPES buffer (pH 7.4), supplemented with 8 mM glucose and 0.5 g/liter BSA and then preincubated for 30 min in 200 µl of the same medium. The medium was removed and 200 µl of fresh buffer containing 20 µl of serum for TSH measurement and 25 µM Rolipram, a cAMP phosphodiesterase inhibitor, were added. The incubation was continued for 1 h, at the termination of which the medium was discarded and replaced with 0.1 M HCl. cAMP was measured in the dried cell extract by RIA according to the method of Brooker (Brooker *et al.* 1979). Blanks were prepared as above but contained 20 µl of human serum without TSH. Thus, this assay measures the stimulus to which the cells are exposed, which reflects both the concentration of the hormone and its specific activity, ie its glycosylation level.

Histology

Thyroid glands were removed from 3 week-old mice and overnight fixed at room temperature in 3.7% formaldehyde. They were dehydrated through isopropanol series, cleared in Histoclear (National Diagnostics, UK), embedded in paraffin and cut at 7-µm. For cryo-sectioning, thyroids were fixed overnight at 4°C in 4% paraformaldehyde in HBS, overnight treated at 4°C in 30% sucrose in HBS, embedded in OCT compound (Klinipath, The Netherlands) and cut at 5-µm. For histological analysis, slides were stained with hematoxylin / eosin (Klinipath, The Netherlands). ImageJ software was used to quantify follicle area as well as cell and follicle densities from a minimum of 5 mice per genotype. For the follicle area, more than 20 follicles were measured in each thyroid gland. For each mouse, cell and follicle density per mm^2 was estimated by counting number of cells and follicles in total area of 0.1 mm^2. Colloid and epithelial areas and volumes as well as the Thyroid Activation Index were obtained as described (Kmiec *et al.* 1998).

Immunohistochemistry

For thyroglobulin (TG) analysis, sections were deparaffinised and treated with 0.3% hydrogen peroxide in methanol for 30 minutes. They were incubated with blocking solution (10% goat serum in PBS) for 1 hour and then with a human TG antibody (Dako, Belgium) diluted 1:2500 overnight at room temperature.

For iodinated TG analysis, quenching endogenous peroxidases was performed, and then antigen retrieval was done by boiling the slides immersed in citrate buffer pH6. They were incubated with blocking solution (10%BSA/2% sheep serum in PBS) for 1 hour and then with an iodinated TG antibody (C.Ris-Stalpers, The Netherlands) diluted 1:2000 overnight at 4°C.

For sodium/iodide symporter (NIS) analysis, sections were permeabilized 20 minutes in PBS - 0.1% Triton and treated with 0.3% hydrogen peroxide for 30 minutes. They were incubated with blocking solution (1% BSA, 2% goat serum in PBS) for 30 minutes and then

with a NIS antibody (a kind gift from Professor Carrasco, Albert Einstein College of Medicine, NY, USA) diluted 1:500 overnight at room temperature.

Semiquantitative PCR

Total RNA was isolated from thyroid tissues using RNeasy Kit (Qiagen, Venlo, Netherlands) including a DNase treatment and was reverse transcribed with the M-MLV Reverse Transcriptase (Invitrogen, Carlsbad, NM) using 300 ng total RNA. The following genes were PCR amplified using sense and antisense oligonucleotide primers as follows: V-abl Abelson murine leukemia viral oncogene homolog 1 (Abl) sense, 5'-TCGGACGTGTGGGCATTT -3', and antisense, 5'-CGCATGAGCTCGTAGACCTTC -3'; Kif3a sense, 5'-ATGCCGATCAATAAGTCGGAGA-3', and antisense, 5'-GTTCCCCTCATTTCATCCACG-3'; NIS sense, 5'-CGCTACGGTCTCAAGTTTCTG-3', and antisense, 5'-CGCAGTTCTAGGTACTGGTAGG-3'. The reaction mixtures contained 5µl PCR buffer 10x (containing 15 mM $MgCl_2$, Qiagen), 1µl DNTP mix (10 mM each DNTP), 1 µl forward primer (10 µM), 1µl reverse primer (10 µM), 2 U Taq DNA polymerase (Qiagen, Venlo, Netherlands), 15 ng template cDNA and RNase-free water to a final volume of 50 µl.

Quantitative PCR

Total RNA from thyroid tissues was isolated using RNeasy Kit (Qiagen, Venlo, Netherlands) including a DNase treatment and was reverse transcribed with the M-MLV Reverse Transcriptase (Invitrogen, Carlsbad, NM) using 120 ng total RNA. Reactions for the quantification of Kif3a, NIS (or Slc5a5), Dio2, TSHr, Gnas1, Adcy 3, 6 and 9, Prkar1 a and b, Prkar2 a and b, and Prkac a and b mRNAs were performed in a CFX96 Real-Time System (Bio-Rad), using SYBR Green as detector dye. PBGD and 36B4 were used as reference genes. The reaction mixtures contained 10 µl SYBR Green PCR Kit (Bio-Rad), 200 nM of each primer, 6 ng template cDNA and RNase-free water to a final volume of 20 µl. The sequences of all oligonucleotide primers are listed in Supplementary Table 1.

Ex vivo thyroid cAMP measurement

Thyroids were washed with cold PBS. Then, they were incubated for 80 minutes (37°C, 5% CO_2) with 900 µl Krebs-Ringer-Bicarbonate buffer (pH 7.4) containing 50 µM Rolipram, a cAMP phosphodiesterase inhibitor. Finally, 100 µl 1M HCl were added and the incubation was continued for 5 minutes. cAMP was measured by RIA (Brooker *et al*. 1979).

In vitro MEF cAMP measurement

The day before the experiment, MEF cells (10^5) were seeded in 3.5-cm diameter dishes with 2 ml culture medium. Before the experiment, the culture medium was removed and cells were rinsed with 1 ml Krebs-Ringer-Bicarbonate buffer (KRB), then preincubated for 30 min in this buffer containing 50 µM Rolipram at 37°C-5%CO_2. The buffer was then removed and replaced with fresh KRB buffer supplemented with 50 µM Rolipram and the different agonists: 10 µM isoproterenol (Sigma-Aldrich, St. Louis, MO) or 10 µM forskolin (Sigma-Aldrich, St. Louis, MO). At the end of the 10 min incubation, the medium was

removed and 1 ml 0.1 M HCl was added to the dishes. cAMP was measured by RIA (Brooker *et al*. 1979).

Flow cytometry

The day before the experiment, MEF cells (10^5) were seeded in 3.5-cm diameter dishes with 2 ml culture medium. Cells were washed with PBS, incubated for 20 min with PBS -EDTA 5 mM on ice and collected. After centrifugation, cells were re-suspended in FACS buffer (PBS, 0.1% BSA, 0.1% sodium azide). For the permeabilization, cells were incubated for 30 min in PBS-2% PFA and then for 3 min in PBS-0.1% NP40. A rabbit antibody directed to β2 adrenergic receptor (dilution 1/50, AbCam, UK) was added and cells were incubated for 1 hour at room temperature. Cells were washed and incubated for 30 minutes on ice with an antibody directed against rabbit Ig coupled to Alexa fluor 488 (dilution 1/1000, Invitrogen, Carlsbad, NM). After washing, cells were resuspended in FACS buffer and analysed on a Cytomics FC500 cytometer (Beckman Coulter).

Statistics

All results are expressed as mean ± SEM and statistical analysis was done by Unpaired *t* test or Mann-Whitney test, using Graph Pad Prism.

Results

Kif3a inactivation in mouse thyroid cells

The Cre recombinase tissue specificity and efficiency at the Kif3a locus were investigated in $Kif3a^{flox/+}$ and $Kif3a^{flox/+}$ $Pax8^{Cre/+}$ mice at the DNA level (Figure 1A and 1B). Three oligonucleotide primers were designed to amplify the wild type, flox and exon 2-deleted (or Δ) Kif3a alleles in the same PCR. As expected, in $Kif3a^{flox/+}$ mice, amplicons of 360 bp and 490 bp, corresponding to the wild type and the flox alleles, respectively, were amplify out of the DNA extracted from 8 different tissues. In $Kif3a^{flox/+}$ $Pax8^{Cre/+}$ mice, an additional 200bp Δ signal was specifically detected after amplification of DNA extracted from the thyroid and the kidney (Figure 1B). The presence of the Δ signal in these two tissues was associated with a decreased intensity of the flox allele signal. These results demonstrate that the floxed Kif3a locus is efficiently recombined by the Cre enzyme. They also confirm previous report indicating that the Cre recombinase is expressed in thyrocytes and kidney cells of $Pax8^{Cre/+}$ mice.

In order to investigate the role of the molecular motor component Kif3a in mouse thyrocytes, $Kif3a^{\Delta/+}$ $Pax8^{Cre/+}$ mice were crossed with $Kif3a^{flox/+}$ mice to produce $Kif3a^{\Delta/flox}$ $Pax8^{Cre/+}$ “mutant” mice, $Kif3a^{+/+}$ and $Kif3a^{flox/+}$ “control” mice as well as $Kif3a^{+/+}$ $Pax8^{Cre/+}$ “Cre” mice from the same litter. RT-PCR, qPCR and Western blot analyses demonstrated a severely reduced Kif3a mRNA and protein in the thyroid of mutant mice, as compared with control and Cre mice (Figure 1C–E).

Normal thyroid migration but hypothyroidism in mutant mice

Mice with all possible genotypes were recovered at Mendelian frequency at birth, suggesting that Kif3a deletion in Pax8-expressing cells is not embryonic lethal. Nevertheless, at

weaning around 3 weeks of age, all mutant mice died. Dying mutant mice presented mild growth retardation and autopsy revealed a marked increase in kidney weight and size, compared with control and Cre mice (Figure S1A, B, C and D). Histological analysis demonstrated the presence of numerous and large cysts in the kidney of mutant mice, providing a probable cause for their reduced survival (Figure S1E). Indeed, in $Pax8^{Cre/+}$ mice, the Cre recombinase is also expressed in kidney cells, and this was confirmed by the presence of severely decreased Kif3a mRNA and protein levels in mutant kidney (Figure S1F and G). No obvious alteration was detected in other organs, including the brain (data not shown). In 3 week-old mutant mice, the thyroid was normally localized in the neck and of normal size and weight (Figure 2A and data not shown). Mutant mice displayed hypothyroidism with low total T4 level and increased TSH bioactivity, as compared with control and Cre mice (Figure 2B and C). No difference was observed in total T3 level between groups of mice (Figure 2B). Interestingly, Cre mice, which are knock-in mice with a heterozygous insertion of the Cre cDNA into exon 3 of the Pax8 gene, presented a mild but significant increase in TSH bioactivity, as compared with control mice. However, in these mice, TSH bioactivity was still markedly below the level observed in mutant mice (Figure 2C). Together, our results indicate that Kif3a inactivation using $Pax8^{Cre/+}$ mice result in early lethality, probably a consequence of kidney failure. Importantly, they indicate that Kif3a inactivation in thyroid follicle cells leads to mild hypothyroidism. They also suggest that, on the genetic background studied, $Pax8^{Cre/+}$ mice have a mild thyroid dysfunction leading to a slight increase in bioactive TSH level.

Normal thyroid structure, but reduced thyroglobulin iodination and NIS expression in the thyroid of mutant mice

Histological examination of 3 week-old thyroids revealed that the general thyroid architecture as well as the follicle and cell densities were normal in Cre and mutant mice (Figure 2D and Figure 3A). A trend for decreased follicular area (Cre mice: 2049 ± 428 μm^2; mutant mice: 1394 ± 135 μm^2; n = 5 mice per group; P = 0.2186), colloid area (Cre mice: 927 ± 230 μm^2; mutant mice: 607 ± 111 μm^2; n = 5 mice per group; P = 0.2469), colloid volume (Cre mice: 46 ± 17 mm^3; mutant mice: 25 ± 7 mm^3; n = 5 mice per group; P = 0.2742), epithelial area (Cre mice: 1121 ± 202 μm^2; mutant mice: 787 ± 33 μm^2; n = 5 mice per group; P = 0.1770), and epithelial volume (Cre mice: 74 ± 21 mm^3; mutant mice: 42 ± 3 mm^3; n = 5 mice per group; P = 0.0952) was observed in mutant thyroids, but the differences did not reach statistical significance when compared with Cre thyroids. A similar Thyroid Activation Index was found in Cre and mutant mice (Cre mice: 1.891 ± 0.2952; mutant mice: 2.090 ± 0.3541; n = 5 mice per group; P = 0.6772). As compared with control and Cre thyroids, thyroglobulin (Tg) mRNA and protein were normal in mutant thyroid, but iodinated TG level in the colloid was significantly decreased in mutant mice, showing a very heterogeneous expression in the different follicles (Figure 3B, 3C and data not shown). In order to define a potential mechanism of this iodination defect, the expression of NIS, the sodium/iodide symporter responsible for the basal membrane iodide uptake, was investigated at the protein and the mRNA levels (Figure 3D–F). NIS protein expression and mRNA level were markedly decreased in mutant mice, as compared with control and Cre mice, reaching about 20% of control level and 40% of Cre level. As expected from

$Pax8^{Cre/+}$ mice, which are heterozygous at the Pax8 locus, a slight but significant decrease in both NIS protein and mRNA levels was observed in these mice.

Together, our results define a marked thyroid dysfunction in mutant mice. This dysfunction is probably a consequence of the nearly complete Kif3a inactivation combined with the partial Pax8 gene inactivation, since mild thyroid alterations are already present in the $Pax8^{Cre/+}$ mice used to inactivate Kif3a in thyroid follicle cells. They also suggest a potential role of the TSH/cAMP signaling pathway in the pathogenesis of the mutant phenotype since NIS mRNA expression, which is altered in mutant mice, is known to be regulated by this pathway in thyroid follicle cells.

Altered TSH signaling pathway in mutant mice

Since NIS mRNA was found significantly decreased in mutant thyroid, mRNA level of other genes known to be involved in or induced by the TSH/cAMP signaling pathway was investigated by qPCR in thyroid of mutant, control and Cre mice (Figures 4 and 5). Out of the genes tested, only mRNA level of Adcy3, the adenylate cyclase 3 gene, of Prkar2b, the PKA regulatory subunit 2b gene, and of Dio2, the type 2 iodothyronine deiodinase gene, were found significantly decreased in mutant thyroid, as compared with control and Cre thyroids. Expression of Dio1, the type1 iodothyronine deiodinase gene, was decreased both in Cre and mutant thyroids, suggesting that Dio1 mRNA may be controlled directly or indirectly by PAX8 transcription factor. By contrast, mRNA level for the TSH receptor, G alpha s, adenylate cyclases 6 and 9, the PKA a and b catalytic subunits as well as for the PKA 1a, 1b and 2a regulatory subunits were similar in mutant, Cre and control thyroids (Figure 5). Interestingly, among the genes tested, only NIS, Adcy3, Prkar2b and Dio2 mRNA expression are known to be regulated by the second messenger cAMP, through CREB transcription factor. Thus, we next investigated basal cAMP level in mutant, Cre and control thyroids (Figure 6). In Cre thyroids, basal cAMP level was significantly increased, as compared to control thyroids. This is most probably the consequence of the increased TSH bioactivity observed in these mice (Figure 2C). Based on this result, basal cAMP level should be markedly increased in mutant thyroids, since TSH bioactivity was about 7 and 4 fold-increased in these mice compared with control and Cre mice, respectively. However, in agreement with a defect in the proximal part of the TSH/cAMP signaling pathway, cAMP level in mutant mice was found only slightly increased when compared with control mice, and severely decreased when compared with Cre mice (Figure 6).

Together, our results suggest that mutant mice present a defect in the proximal part of the TSH/TSHreceptor/cAMP signaling pathway. They also confirm that the $Pax8^{Cre/+}$ mice used to induce recombination have a thyroid dysfunction which is compensated by increased TSH bioactivity.

Abnormal plasma membrane GPCR transport in $Kif3a^{-/-}$ mouse embryonic fibroblasts

The faint TSH receptor expression on mouse thyroid follicle cells and/or the absence of adequate antibody directed against this receptor did not allow us to clearly localize or quantify the TSH receptor on the follicle cell basal membrane and to validate *in vivo* our hypothesis concerning the defect in the proximal part of the TSH/TSH receptor/cAMP

signaling pathway in mutant mice (data not shown). We thus used a less complex cellular model to probe this hypothesis: Kif3a$^{-/-}$ mouse embryonic fibroblasts (MEF) infected with RFP-tagged TSH receptor-expressing lentiviruses. Unfortunately, infections demonstrated that both RFP-TSH receptor mRNA and protein were very significantly less expressed in Kif3a$^{-/-}$ than in Kif3a$^{+/+}$ MEF, preventing the use of lentivirus to probe our hypothesis (data not shown). As an experimental surrogate, we decided to study the subcellular localization and signaling downstream of another G protein coupled receptor (GPCR) naturally expressed by MEF : the β2 adrenergic receptor. Indeed, this receptor belongs to the same GPCR subclass as the TSH receptor and is similarly expressed in Kif3a$^{+/+}$ and Kif3a$^{-/-}$ MEF (Figure 7A). Despite the similar protein expression when tested by Western blotting on MEF protein extracts, a significantly reduced β2 adrenergic receptor expression was detected by flow cytometry at the cell surface in Kif3a$^{-/-}$ cells (Figure 7B). Therefore, in response to stimulation by isoproterenol, a β2 adrenergic receptor agonist, significantly lower cAMP levels were observed in Kif3a$^{-/-}$ MEF, as compared with Kif3a$^{+/+}$ MEF (Figure 7C). Altogether, these results suggest that the absence of Kif3a leads to alterations in β2 adrenergic GPCR transport to the plasma membrane and to defective downstream signalling.

Discussion

We report here for the first time that 3 week-old Pax8$^{Cre/+}$ mice present minor thyroid functional alterations and that inactivation of Kif3a, a kinesin 2 molecular motor subunit, with these Cre mice results in a mild hypothyroidism at 3 weeks of age, probably secondary to defects in TSH receptor signaling. This mild hypothyroidism is characterized by a decreased circulating T4 and an increased TSH level, a probable consequence of a reduced production of intracellular T3 from T4 in pituitary cells. Our results also indicate that lack of Kif3a in cells leads to a decreased cell surface expression of the endogenous β2 adrenergic receptor and a decreased signaling in response to stimulation.

In man, at least 10 different mutations have been identified in the PAX8 gene, leading to thyroid dysgenesis and congenital hypothyroidism (Meeus *et al*. 2004; Montanelli & Tonacchera 2010). All affected people are heterozygous for the PAX8 mutation and transmission is autosomal dominant (Meeus *et al*. 2004; Montanelli & Tonacchera 2010). Unexpectedly, no structural or functional thyroid defect have been previously reported in Pax8$^{Cre/+}$ mice, suggesting that, in this species, the presence of one functional Pax8 allele is sufficient for normal organogenesis and function (Amendola *et al*. 2005). Unlike published data on these mice, we show here that Pax8$^{Cre/+}$ mice present minor thyroid functional defects, including a significant decrease in NIS mRNA expression, resulting in a slight compensatory increase in circulating TSH and intracellular cAMP levels, sufficient to maintain blood T4 levels in the normal range. The discrepancy between our results and those reported by Amendola (normal TSH and T4 levels) may be explained by a difference in the mouse genetic background and/or in dietary level of iodine. These findings certainly complicate the interpretation of our results on the role of Kif3a in the thyroid.

It has been extensively demonstrated that the kinesin 2 molecular motor, including Kif3a, is essential for correct primary cilium assembly (Rosenbaum & Witman 2002). Indeed, Kif3a

participates to the intraflagellar transport in this antenna-like structure and Kif3a inactivation in mice leads to absence of primary cilium at the cell surface and developmental alterations characteristic of ciliopathies (Marszalek *et al*. 1998; Lin *et al*. 2003). Antenna-like structures related to primary cilium have been detected on thyroid cells during development and on mature follicular cells, but major differences exist between species (Sobrinho-Simões & Johannessen 1981). In adult mouse, it has been reported that only 2% of thyroid cells present a cilium, and its precise role has not been addressed so far (Wetzel & Wollman 1969). We were unable to detect an acetylated α-tubulin positive primary cilium on thyroid cells in mouse at embryonic or adult stages (data not shown). However, we show here that Kif3a inactivation from E8.5 in the thyroid bud had no obvious effect on thyroid development and migration, suggesting that Kif3a and potential primary cilium have no essential role in these processes, at least in mouse.

Correct cell surface expression of receptors, including TSH and β2 adrenergic GPCR, is essential for binding of water-soluble ligand and for initiating downstream intracellular signaling. In MEF in the absence of any Pax8 gene alteration, our results clearly indicate that Kif3a inactivation leads to significantly lower β2 adrenergic receptor expression at the cell surface and, as a consequence, to markedly decreased downstream signaling in response to agonist stimulation. The kinesin 2 molecular motor is known to participate to “non intraflagellar” transport in the cell, like retrograde traffic between the Golgi and the endoplasmic reticulum (ER) (Stauber *et al*. 2006), endosome and lysosome transports (Bananis *et al*. 2004; Brown *et al*. 2005), endocytosis and recycling of cell surface receptors like transferrin, cubulin and megalin receptors, or of other proteins like Clc-5, the H^+/Cl^- exchange transporter (Schonteich *et al*. 2008; Reed *et al*. 2010). The KIF3 molecular motor also plays an important role in the transport of vesicles containing GluR2 and GLUT4 receptors or MT1-MMP and MMP-9 metalloproteinases from the cytosol to the plasma membrane (Imamura *et al*. 2003; Wiesner *et al*. 2010; Hanania *et al*. 2012; Lin *et al*. 2012). Unfortunately, we were unable to analyze the intracellular traffic or the cell surface expression of the TSH receptor *in vivo* or *in vitro*, due to the lack of specific antibody working on tissue sections (and probably also to the very low expression of the TSH receptor at the thyrocyte surface) and the unexpected consequence of Kif3a inactivation on TSH receptor expression directed by lentivirus infection. Given that the TSH and the β2 adrenergic receptors belong to the same subclass of GPCR and have similar post-translational modifications (glycosylation, sialylation and palmitoylation), we speculate here that they use similar mechanisms for transport from the Golgi to the plasma membrane and/or for recycling at the cell surface. Thus, based on our *in vitro* results on the β2 adrenergic receptor in Kif3a deficient MEF, we suggest that Kif3a inactivation in thyrocytes may lead to altered transport and/or recycling of the TSH receptor, decreased expression at the basolateral membrane and altered TSH signaling. TSH signaling is clearly altered in $Kif3a^{\Delta/flox}$ $Pax8^{Cre/+}$ mutant mice. First the expression of specific genes controlled by cAMP through CREB transcription factor, like NIS, Adcy3, Prkar2b and Dio2, are significantly decreased in these mice. Second, as compared with thyroid of Cre mice, the cAMP levels in mutant thyroid are markedly lower. Thereby mutant mice are not able to compensate a thyroid dysfunction despite of increased TSH bioactivity, unlike Cre mice. Our mutant phenotype is indeed reminiscent of the phenotype observed in TSH receptor

deficient mice. In the latter mice, normal thyroid development is also associated with TSH resistance, decreased NIS mRNA expression and congenital hypothyroidism (Postiglione *et al.* 2002). However, our mutant phenotype is less pronounced than the TSH receptor deficient phenotype. As for the β2 adrenergic receptor in Kif3a$^{-/-}$ MEF, it is probable that a significant fraction of the TSH receptor is still expressed at the thyrocyte cell surface and functional. Partial compensation of kinesin 2 deficiency by other kinesins, like Kinesin 1 which is expressed in thyrocytes (data not shown), to carry cargo to their final destination is abundantly described in the literature (Brown *et al.* 2005; Hirokawa *et al.* 2009; Wiesner *et al.* 2010). It is noteworthy here that mice were analyzed only at 3 weeks of age, given the experimental difficulties to record similar data earlier in mouse. The thyroid phenotype of Kif3a$^{\Delta/flox}$ Pax8$^{Cre/+}$ mutant mice is thus unknown at earlier developmental stages and it could eventually change with age, as reported in type 3 deiodinase knockout mice (Hernandez *et al.* 2006). Furthermore, the Kif3a mutation analyzed here is not strictly thyrocyte-specific and the mice have a severe kidney phenotype which probably explains the post-natal lethality. Severe chronic kidney disease in man results in decreased circulating T4, T3 and TSH levels, a consequence of changes in peripheral hormone metabolism, thyroid hormone binding proteins and central defects (van Hoek & Daminet 2009). Although the consequences of chronic kidney disease have not been clearly reported in the literature for 3 week-old mice, the human phenotype is not identical to the Kif3a$^{\Delta/flox}$ Pax8$^{Cre/+}$ mouse phenotype where only T4 level is decreased and where increased TSH level is associated with low thyroid cAMP level and with altered expression of specific genes controlled by cAMP, which together sign the presence of TSH signalling defects.

In conclusion, our results in 3 week-old Kif3a$^{\Delta/flox}$ Pax8$^{Cre/+}$ mutant mice indicate first that the Pax8$^{Cre/+}$ mice used in these experiments present minor thyroid functional defects resulting in a slight increase in circulating bioactive TSH and intracellular cAMP levels, presumably allowing to maintain blood T4 levels in the normal range. Second, Kif3a invalidation in thyrocytes markedly amplifies the phenotype observed in Pax8$^{Cre/+}$ mice, resulting in an altered TSH signaling upstream of the second messenger cAMP and a mild hypothyroidism 3 weeks after birth. Finally, our results in MEF indicate that Kif3a inactivation in the absence of any Pax8 gene alteration leads to altered β2 adrenergic GPCR plasma membrane expression; we suggest that a similar mechanism may explain the altered TSH signaling and mild hypothyroidism observed in Kif3a$^{\Delta/flox}$ Pax8$^{Cre/+}$ mutant mice. In future genetic studies on congenital hypothyroidism or high TSH serum level, it will be important to look for variants in the Kif3a gene.

Supplementary Material

Refer to Web version on PubMed Central for supplementary material.

Acknowledgements

We thank D. Christophe for discussion, S. Costagliola for antibodies, L. S. Goldstein for the Kif3a$^{delta/flox}$ mice, and M. Busslinger for the Pax8$^{Cre/+}$ mice.

Funding: This work was supported by the Fonds de la Recherche Scientifique-FNRS (FRS-FNRS to S. S.), the Fonds de la Recherche Scientifique Médicale (FRSM ; to S. S.), the Fondation Rose et Jean Hoguet and the Fonds David et Alice Van Buuren (to E. D'A.).

Abbreviations

MEF	mouse embryonic fibroblast
TSH	thyroid stimulating hormone
cAMP	cyclic adenosine monophosphate
NIS	sodium/iodide symporter, encoded by the Slc5a5 gene
TG	thyroglobulin
I TG	iodinated thyroglobulin
KRB	Krebs-Ringer bicarbonate
HBS	HEPES-buffered saline
PBGD	Porphobilinogen deaminase
36B4	acidic ribosomal phosphoprotein P0
qPCR	quantitative PCR
Prkar2b	regulatory subunit 2b of PKA
PFA	paraformaldehyde
ADRB2	β2 adrenergic receptor
GPCR	G protein coupled receptor

References

Amendola E, De Luca P, Macchia PE, Terracciano D, Rosica A, Chiappetta G, Kimura S, Mansouri A, Affuso A, Arra C, Macchia V, Di Lauro R, De Felice M. A mouse model demonstrates a multigenic origin of congenital hypothyroidism. Endocrinology. 2005; 146:5038–47. [PubMed: 16150900]

Bananis E, Nath S, Gordon K, Satir P, Stockert RJ, Murray JW, Wolkoff AW. Microtubule-dependent movement of late endocytic vesicles in vitro: requirements for Dynein and Kinesin. Molecular Biology of the Cell. 2004; 15:3688–97. [PubMed: 15181154]

Bouchard M, Souabni A, Mandler M, Neubüser A, Busslinger M. Nephric lineage specification by Pax2 and Pax8. Genes & Development. 2002; 16:2958–70. [PubMed: 12435636]

Bouchard M, Souabni A, Busslinger M. Tissue-specific expression of cre recombinase from the Pax8 locus. Genesis. 2004; 38:105–9. [PubMed: 15048807]

Brooker G, Harper JF, Terasaki WL, Moylan RD. Radioimmunoassay of cyclic AMP and cyclic GMP. Advances in Cyclic Nucleotide Research. 1979; 10:1–33. [PubMed: 222120]

Brown CL, Maier KC, Stauber T, Ginkel LM, Wordeman L, Vernos I, Schroer TA. Kinesin-2 is a motor for late endosomes and lysosomes. Traffic. 2005; 6:1114–24. [PubMed: 16262723]

Hanania R, Song Sun H, Xu K, Pustylnik S, Jeganathan S, Harrison RE. Classically activated macrophages use stable microtubules for matrix metalloproteinase-9 (mmp-9) secretion. Journal of Biological Chemistry. 2012; 287:8468–83. [PubMed: 22270361]

Hernandez A, Martinez ME, Fiering S, Galton VA, St Germain D. Type 3 deiodinase is critical for the maturation and function of the thyroid axis. Journal of Clinical Investigation. 2006; 116:476–484. [PubMed: 16410833]

Hirokawa N. Stirring up development with the heterotrimeric kinesin KIF3. Traffic. 2000; 1:29–34. [PubMed: 11208056]

Hirokawa N, Noda Y, Tanaka Y, Niwa S. Kinesin superfamily motor proteins and intracellular transport. Nature Reviews Molecular Cell Biology. 2009; 10:682–96.

Imamura T, Huang J, Usui I, Satoh H, Bever J, Olefsky JM. Insulin-induced GLUT4 translocation involves protein kinase C-lambda-mediated functional coupling between Rab4 and the motor protein kinesin. Molecular and Cellular Biology. 2003; 23:4892–900. [PubMed: 12832475]

Kmiec Z, Kotlarz G, Smiechowska B, Mysliwski A. The effect of fasting and refeeding on thyroid follicule structure and thyroid hormone levels in young and old rats. Archives of Gerontology and Geriatrics. 1998; 26:161–175. [PubMed: 18653134]

Lin F, Hiesberger T, Cordes K, Sinclair AM, Goldstein LS, Somlo S, Igarashi P. Kidney-specific inactivation of the KIF3A subunit of kinesin-II inhibits renal ciliogenesis and produces polycystic kidney disease. Proceedings of the National Academy of Sciences of the United States of America. 2003; 100:5286–91. [PubMed: 12672950]

Lin Y, Jones BW, Liu A, Vazquéz-Chona FR, Lauritzen JS, Ferrell WD, Marc RE. Rapid glutamate receptor 2 trafficking during retinal degeneration. Molecular Neurodegeneration. 2012; 7:7. [PubMed: 22325330]

Marszalek JR, Ruiz-Lozano P, Roberts E, Chien KR, Goldstein LS. Situs inversus and embryonic ciliary morphogenesis defects in mouse mutants lacking the KIF3A subunit of kinesin-II. Proceedings of the National Academy of Sciences of the United States of America. 1999; 96:5043–8. [PubMed: 10220415]

Meeus L, Gilbert B, Rydlewski C, Parma J, Roussie AL, Abramowicz M, Vilain C, Christophe D, Costagliola S, Vassart G. Characterization of a novel loss of function mutation of PAX8 in a familial case of congenital hypothyroidism with in-place, normal-sized thyroid. The Journal of Clinical Endocrinology & Metabolism. 2004; 89:4285–91. [PubMed: 15356023]

Moeller LC, Kimura S, Kusakabe T, Liao XH, Van Sande J, Refetoff S. Hypothyroidism in thyroid transcription factor 1 haploinsufficiency is caused by reduced expression of the thyroid-stimulating hormone receptor. Molecular Endocrinology. 2003; 17:2295–302. [PubMed: 12907760]

Montanelli L, Tonacchera M. Genetics and phenomics of hypothyroidism and thyroid dys- and agenesis due to PAX8 and TTF1 mutations. Molecular and Cellular Endocrinology. 2010; 322:64–71. [PubMed: 20302910]

Nonaka S, Tanaka Y, Okada Y, Takeda S, Harada A, Kanai Y, Kido M, Hirokawa N. Randomization of left-right asymmetry due to loss of nodal cilia generating leftward flow of extraembryonic fluid in mice lacking KIF3B motor protein. Cell. 1998; 95:829–37. [PubMed: 9865700]

Perret J, Ludgate M, Libert F, Gerard C, Dumont JE, Vassart G, Parmentier M. Stable expression of the human TSH receptor in CHO cells and characterization of differentially expressing clones. Biochemical and Biophysical Research Communications. 1990; 171:1044–50. [PubMed: 2171505]

Plachov D, Chowdhury K, Walther C, Simon D, Guenet JL, Gruss P. Pax8, a murine paired box gene expressed in the developing excretory system and thyroid gland. Development. 1990; 110:643–51. [PubMed: 1723950]

Postiglione MP, Parlato R, Rodriguez-Mallon A, Rosica A, Mithbaokar P, Maresca M, Marians RC, Davies TF, Zannini MS, De Felice M, Di Lauro R. Role of the thyroid-stimulating hormone receptor signaling in development and differentiation of the thyroid gland. Proceedings of the National Academy of Sciences of the United States of America. 2002; 99:15462–7. [PubMed: 12432093]

Reed AA, Loh NY, Terryn S, Lippiat JD, Partridge C, Galvanovskis J, Williams SE, Jouret F, Wu FT, Courtoy PJ, Nesbit MA, Rorsman P, Devuyst O, Ashcroft FM, Thakker RV. CLC-5 and KIF3B interact to facilitate CLC-5 plasma membrane expression, endocytosis, and microtubular transport: relevance to pathophysiology of Dent's disease. American Journal of Physiology - Renal Physiology. 2010; 298:F365–80. [PubMed: 19940036]

Rosenbaum JL, Witman GB. Intraflagellar transport. Nature Reviews Molecular Cell Biology. 2002; 3:813–25.

Scholey JM. Kinesin-II, a membrane traffic motor in axons, axonemes, and spindles. Journal of Cellular Biology. 1996; 133:1–4.

Schonteich E, Wilson GM, Burden J, Hopkins CR, Anderson K, Goldenring JR, Prekeris R. The Rip11/Rab11-FIP5 and kinesin II complex regulates endocytic protein recycling. Journal of Cell Sciences. 2008; 121:3824–33.

Sobrinho-Simões M, Johannessen JV. Scanning electron microscopy of the normal human thyroid. Journal of Submicroscopic Cytology. 1981; 13:209–22. [PubMed: 7338967]

Stauber T, Simpson JC, Pepperkok R, Vernos I. A role for kinesin-2 in COPI-dependent recycling between the ER and the Golgi complex. Current Biology. 2006; 16:2245–51. [PubMed: 17113389]

Van Hoek I, Daminet S. Interactions between thyroid and kidney function in pathological conditions of these organ systems. General and Comparative Endocrinology. 2009; 160:205–2015. [PubMed: 19133263]

Wetzel BK, Wollman SH. Fine structure of a second kind of thyroid follicle in the C3H mouse. Endocrinology. 1969; 84:563–78. [PubMed: 5773158]

Wiesner C, Faix J, Himmel M, Bentzien F, Linder S. KIF5B and KIF3A/KIF3B kinesins drive MT1-MMP surface exposure, CD44 shedding, and extracellular matrix degradation in primary macrophages. Blood. 2010; 116:1559–69. [PubMed: 20505159]

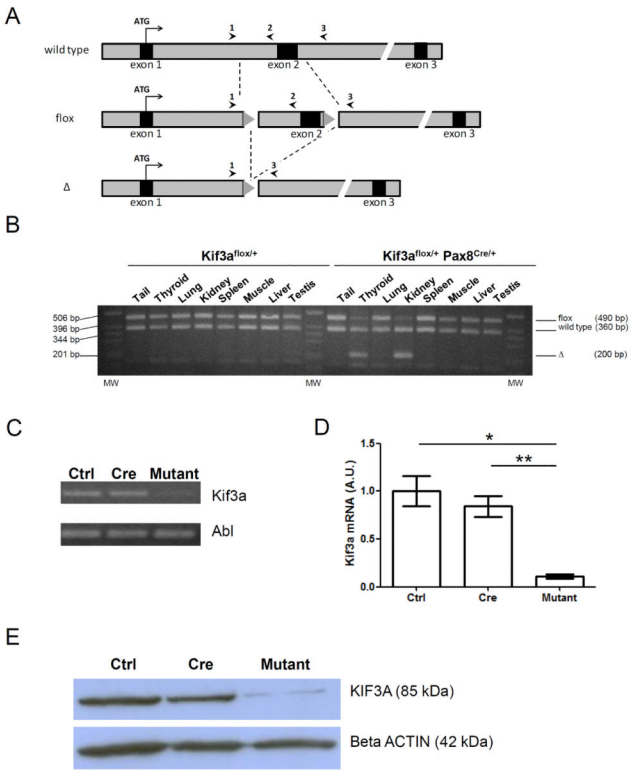

Figure 1. Strategy to inactivate Kif3a in thyroid follicle cells

(**A**) Mice with a wild type, a floxed and/or a delta (Δ) Kif3a allele were used in the study. Black boxes: exons of the Kif3a gene; triangles: loxP sites; arrowheads: primers used to identify the mouse genotype in PCR. (**B**) Gel electrophoresis of a PCR performed on DNA extracted from different tissues of $Kif3a^{flox/+}$ and $Kif3a^{flox/+}$ $Pax8^{Cre/+}$ mice, using the 3 primers shown in (**A**). Amplicons of 490bp, 360bp and 200bp are identified and correspond to the floxed, wild type and Δ alleles, respectively. The Δ allele is solely present in the thyroid and the kidney. MW: molecular weight. Kif3a mRNA identification and quantification by (**C**) RT-PCR and (**D**) qPCR performed on thyroid cDNA from 3 week-old mice. The Abl gene was used as control in the RT-PCR experiments. In qPCR, means ± SEM of 5 independent experiments are represented. A. U.: arbitrary units. Statistics (*t* test with Welch's correction): *: P<0.05, **: P<0.01. (**E**) Western blot analysis of thyroid protein extracts from 3 week-old normal, Cre and mutant mice with a Kif3a antibody. Beta actin served as loading control.

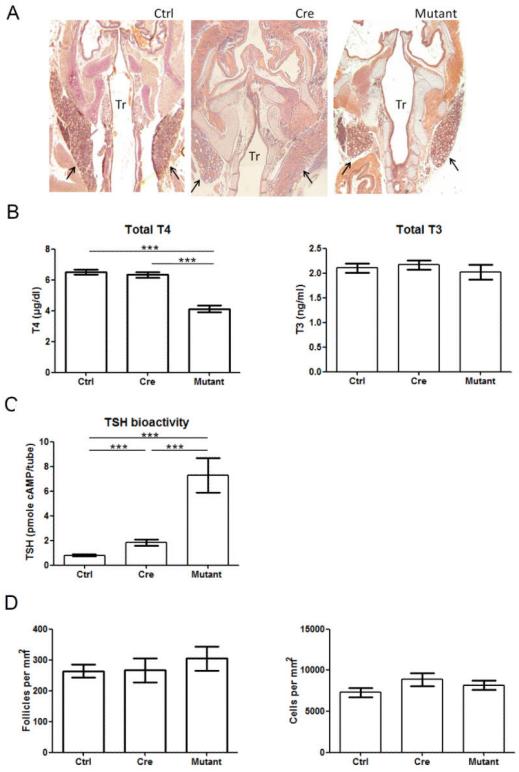

Figure 2. Normal thyroid migration but hypothyroidism in mutant mice

(**A**) Sections through the neck of 3 week-old control, Cre and mutant mice showing the left and right lobes of the thyroid (arrows) and the trachea (Tr). (**B**) Total T4 in the blood of 3 week-old control (n = 71), Cre (n = 59) and mutant (n = 46) mice. Total T3 : control (n = 29), Cre (n = 20) and mutant (n = 17) mice and (**C**) TSH bioactivity : control (n = 75), Cre (n = 63) and mutant (n = 52) mice. Means ± SEM are represented. Statistics (Mann Whitney test): ***: P<0.001. (**D**) Cell and follicle densities were determined in thyroids of 3 week-old control (Ctrl, n = 5 to 11), Cre (n = 5) and mutant (n = 5 to 13) mice. Means ± SEM are represented. No statistical difference was observed between control, Cre and mutant mice.

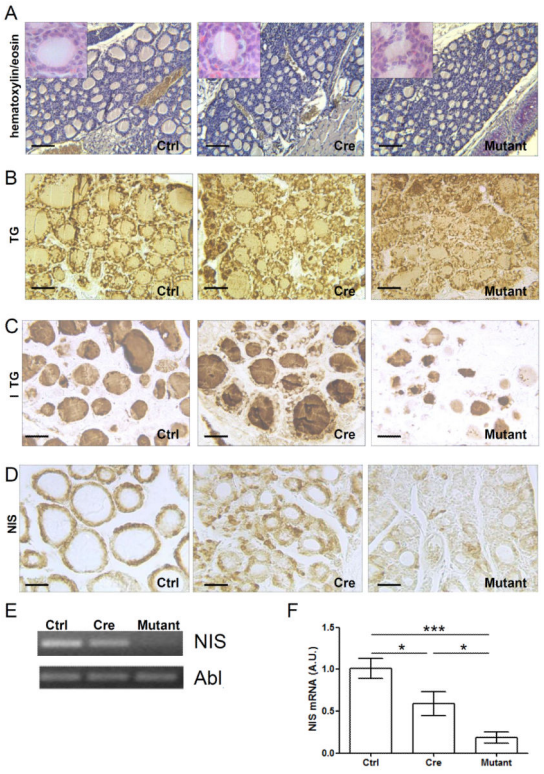

Figure 3. Normal histological structure, but decreased iodinated thyroglogulin and NIS expression in mutant thyroid

(**A**) Hematoxylin/eosin-stained sections of thyroid from 3 week-old control, Cre and mutant mice. Bars: 100 μm. Insets show follicles at higher magnification (x40). Immunodetection of (**B**) thyroglobulin (TG), (**C**) iodinated thyroglobulin and (**D**) NIS proteins on thyroid sections from 3 week-old control, Cre and mutant mice. Bars: 50 μm. NIS mRNA identification and quantification by (**E**) RT-PCR and (**F**) qPCR performed on thyroid cDNA from 3 week-old control, Cre and mutant mice. The Abl gene was used as control in the RT-PCR experiments. In qPCR, means ± SEM of 5 independent experiments are represented. A. U.: arbitrary units. Statistics (Unpaired *t* test): *: P<0.05, ***: P<0.001.

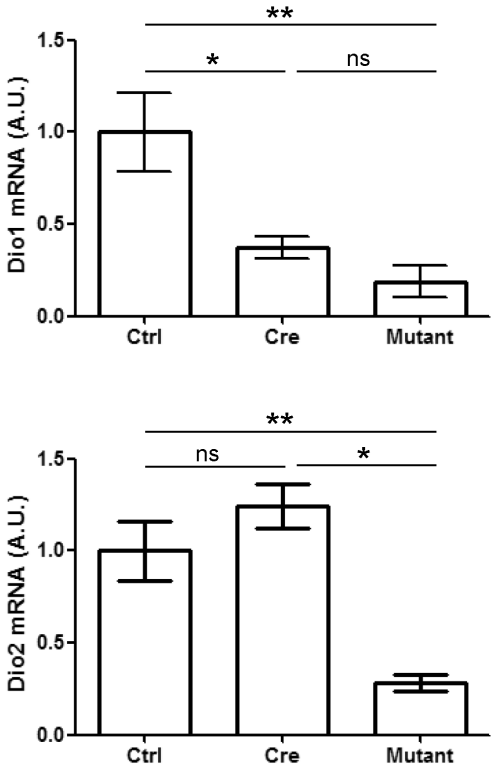

Figure 4. Reduced Dio1 and Dio2 mRNA expression in thyroid of mutant mice

Messenger RNA encoding Dio1 and Dio2 were quantified by qPCR performed on thyroid cDNA from 3 week-old control, Cre and mutant mice. Means ± SEM of 4 or 5 independent experiments are represented. A. U.: arbitrary units. Statistics (Unpaired *t* test or Mann Whitney test): ns (non-significant): P>0.05, *: P<0.05, **: P<0.01. Dio1 : type 1 iodothyronine deiodinase, Dio2 : type 2 iodothyronine deiodinase.

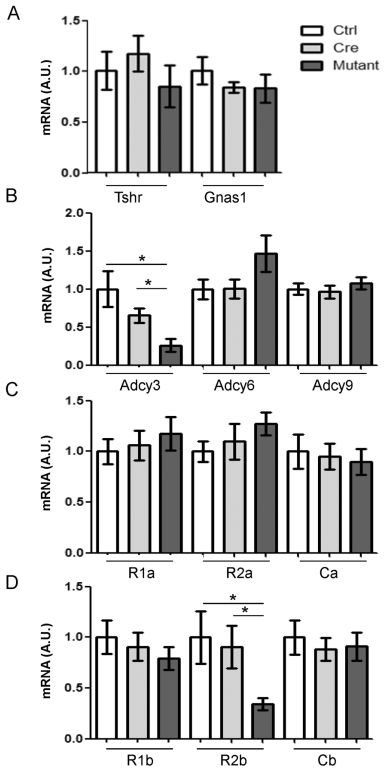

Figure 5. Reduced Adcy3 and Prkar2b mRNA expression in thyroid of mutant mice

Messenger RNA encoding (**A**) Tshr and Gnas1, (**B**) Adcy3, 6 and 9 as well as (**C**) the a and (**D**) the b subunits of Prkar1 (R1a and R1b), Prkar2 (R2a and R2b) and Prkac (Ca and Cb) were quantified by qPCR performed on thyroid cDNA from 3 week-old control, Cre and mutant mice. Means ± SEM of 4 or 5 independent experiments are represented. A. U.: arbitrary units. Statistics (Unpaired *t* test or Mann Whitney test): *: P<0.05. Tshr : TSH receptor, Gnas1 : protein $G_{\alpha s}$, Adcy : adenylate cyclase, Prkar : Protein kinase A regulatory subunit , Prkac : Protein kinase A catalytic subunit.

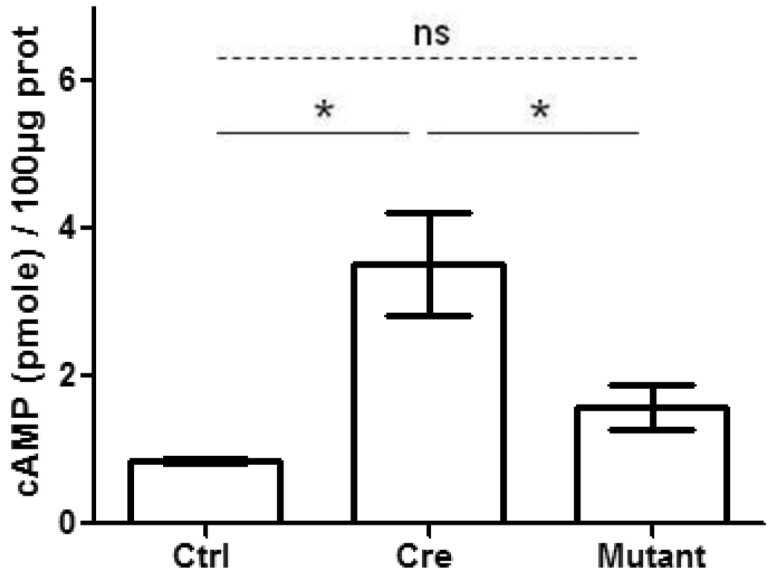

Figure 6. Altered basal cAMP level in thyroid of Cre and mutant mice

Basal cAMP level was analyzed in 3 week-old control (n = 7), Cre (n = 6) and mutant (n = 6) thyroids. Means ± SEM of cAMP levels per 100 µg of thyroid protein extract are represented. Statistics (Mann Whitney test): ns (non-significant): $P>0.05$, *: $P<0.05$.

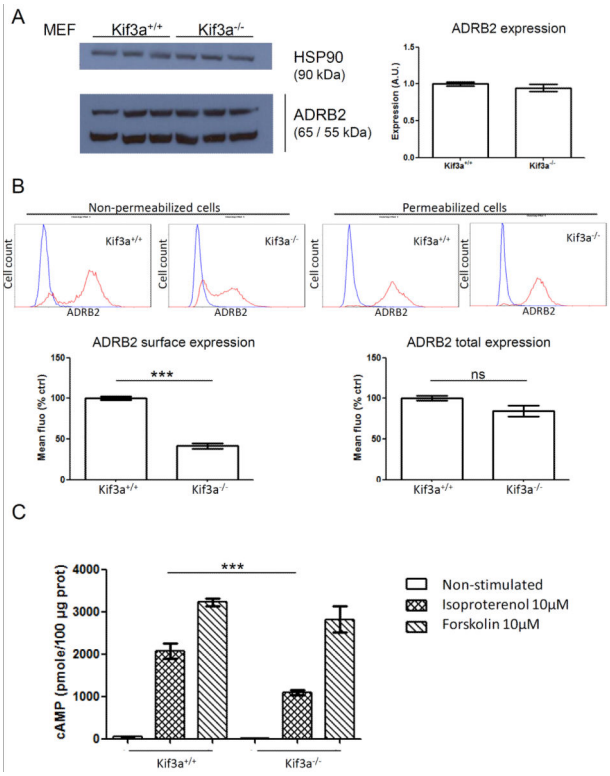

Figure 7. Reduced surface expression and signaling response of β_2 adrenergic receptor in Kif3a$^{-/-}$ cells

Total cellular expression and cell surface expression of the β_2 adrenergic receptor were respectively analyzed (**A**) by western blotting (n= 3) and (**B**) by flow cytometry (n= 8). Red: ADRB2, blue: negative control. (**C**) cAMP levels in response to isoproterenol or forskolin stimulation were determined in Kif3a$^{+/+}$ and Kif3a$^{-/-}$ cells (n= 9). Statistics (Mann Whitney test): ns (non-significant): P>0.05, ***: P<0.001. Adrb2 : β2 adrenergic receptor.